



EXPERIMENTAL AND NUMERICAL INVESTIGATION OF THE EFFECT OF MICROPARTICLE REINFORCEMENT ON MECHANICAL PROPERTIES IN THERMOSET MATRIX COMPOSITES

TERMOSET MATRİS KOMPOZİTLERDE MİKROPARTİKÜL TAKVİYESİNİN MEKANİK ÖZELLİKLER ÜZERİNDEKİ ETKİSİNİN DENEYSEL VE SAYISAL İNCELENMESİ

Görkem ÖZKAN¹  Furkan Giray ÖZKAN²  Mustafa Emre ALTINTAŞ³ 
Aybala USTA⁴  Muhammet CEYLAN⁵ 

<https://doi.org/10.55071/ticaretfdb.1699827>

Corresponding Author
(Sorumlu Yazar)
mceylan@ticaret.edu.tr

Received
(Geliş Tarihi)
17.05.2025

Revised
(Revizyon Tarihi)
07.10.2025

Accepted
(Kabul Tarihi)
09.10.2025

Abstract

In this study, the mechanical characteristics of carbon fiber-epoxy composites containing different ratios of SiO₂ and TiO₂ microparticles in their matrix, produced from nine sheets by hand lay-up, were investigated. The layer orientations of the composites were compared in different configurations and optimized, and the suitable ply sequence [0° / +45° / -45° / 90° / 0° / 90° / -45° / +45° / 0°] was determined. The specimens evaluated within the scope of the experiment were prepared in accordance with ASTM-D638 and ASTM E23 standards, and tensile and Charpy impact tests were performed. Composite plates were fabricated with four different microparticle ratios by mass (0, 1%, 2%, and 4%). In the tensile tests, the composite containing 1% SiO₂-TiO₂ microparticles was observed to exhibit a 4,33% increase in ultimate tensile strength compared to the composite without microparticles. Tensile strength and impact strength data obtained from the tests were compared and presented. The aim of this research was to investigate the effects of adding SiO₂ and TiO₂ microparticles in various ratios on the mechanical properties of the composites. Tensile and Charpy impact tests were used to evaluate these effects.

Keywords: Composite, TiO₂ microparticles, SiO₂ microparticles, mechanical properties, thermoset matrix.

Öz

Bu çalışmada, el yatırması yöntemiyle 9 tabakadan üretilen ve matris içerisinde farklı oranlarda SiO₂ ve TiO₂ mikropartikülleri bulunan karbon fiber-epoksi kompozitlerin mekanik özellikleri incelenmiştir. Kompozitlerin katman yönelimleri farklı dizilimlerde karşılaştırılarak optimize edilmiş ve uygun katman yönelimi [0° / +45° / -45° / 90° / 0° / 90° / -45° / +45° / 0°] olarak belirlenmiştir. Deney kapsamında değerlendirilecek numuneler, ASTM-D638 ve ASTM E23 standartlarına uygun olarak üretilmiş ve çekme ile Charpy darbe testlerine tabi tutulmuştur. Kompozit plakalar, kütlece dört farklı mikropartikül oranıyla (0, %1, %2 ve %4) üretilmiştir. Çekme testlerinde, %1 SiO₂-TiO₂ mikropartikülleri içeren kompozitte, mikropartikül içermeyen kompozite kıyasla nihai çekme dayanımında %4,33'lük bir artış gözlemlenmiştir. Testlerden elde edilen çekme ve darbe dayanım verileri karşılaştırılmış ve sunulmuştur. Bu araştırmanın amacı, SiO₂ ve TiO₂ kombinasyonundan oluşan mikropartiküller farklı oranlarda kompozite eklendiğinde, kompozit malzemenin mekanik özelliklerinde meydana gelen değişimlerin gözlemlenmesi ve araştırılmasıdır. Bu etkilerin araştırılmasında çekme ve Charpy darbe testleri kullanılmıştır.

Anahtar Kelimeler: Kompozit, TiO₂ mikropartiküller, SiO₂ mikropartiküller, mekanik özellikler, termoset matris.

¹Marmara University, Faculty of Engineering, Department of Mechanical Engineering, Istanbul Türkiye. gorkemozkan@marun.edu.tr.

²Marmara University, Faculty of Engineering, Department of Mechanical Engineering, Istanbul, Türkiye. furkan.giray@marun.edu.tr.

³Marmara University, Faculty of Engineering, Department of Mechanical Engineering, Istanbul, Türkiye. mustafaaltintas20@marun.edu.tr.

⁴Marmara University, Faculty of Engineering, Department of Mechanical Engineering, Istanbul, Türkiye. aybala.usta@marmara.edu.tr.

⁵Istanbul Ticaret University, Faculty of Engineering, Department of Mechatronics Engineering, Istanbul, Türkiye. mceylan@ticaret.edu.tr.

1. INTRODUCTION

Engineering and materials science advancements continue at a fast pace. These developments are also seen in the field of composite materials. Innovations in composite materials have enabled the creation of novel composites with enhanced qualities. Among these advances, thermoset matrix composites reinforced with nanoparticles are gaining popularity due to their prospective applications in a variety of industrial sectors, including aerospace, automotive, and construction, thanks to their improved mechanical performance (Han & Yan, 2016; Wang, et al., 2013). This research seeks to examine the impact of introducing particles to composites on their mechanical characteristics (Kim, et al. 2008). The nanoparticles employed in this study will be silicon dioxide (SiO₂) and titanium dioxide (TiO₂).

Thermoset polymers are those produced by the irreversible curing of a soft solid or viscous liquid pre-polymer (Kandelbauer, 2014). Because of their outstanding thermal stability and structural integrity, they are commonly employed as composite material matrices. However, the brittle character and low mechanical strength of these polymers might provide difficulties in some high-performance applications. The thermoset matrix in this study's composite is made of carbon fiber (Zhang, et al., 1993; Heutling, et al., 1998). The use of nanoparticles into thermoset matrices can improve mechanical qualities, addressing issues such as brittleness. Nanoparticles, with their high surface area-to-volume ratios and exceptional physical qualities, can greatly increase composites' mechanical properties such as tensile strength, flexural strength, and impact resistance (Wetzel, et al., 2002).

The influence of nanosilicon dioxide on the mechanical characteristics of carbon fiber reinforced epoxy composites G.S. Researched by Divya and B. Suresha. To improve SiO₂ dispersion, amine-containing liquid rubber was mixed into the epoxy matrix. The SiO₂ was then fully blended using an ultrasonic technique (Suresha, et al., 2021). Hot pressing and vacuum bagging were used to produce a carbon fabric reinforced epoxy (CF/Ep) composite with surface treated nano-SiO₂ (Muda & Mustapha, 2018). Following ASTM recommendations, the effect of silane-treated nano-SiO₂ on static mechanical characteristics such as hardness, tensile, and flexural properties was assessed at filler loadings of 0,5%, 1%, and 3% by weight (Suresha, et al., 2021). According to experimental data, adding a silane coupling agent improves the interfacial interaction between nano-SiO₂ particles and epoxy resin, increasing surface hardness, tensile strength, and bending properties. Furthermore, it was discovered that CF/Ep composites with 3 percent nano-SiO₂ filler had a higher void content (Suresha, et al., 2021).

Silicon dioxide (SiO₂) nanoparticles are known for their high hardness, chemical stability, and heat resistance. Several earlier investigations have indicated that these nanoparticles may improve the mechanical characteristics of composites, making them an excellent alternative for reinforcement (Rong, et al., 2015). TiO₂ nanoparticles, on the other hand, are well-known for their great tensile strength, corrosion resistance, and photocatalytic characteristics (Tutunchi, et al., 2015). It is believed that including SiO₂ and TiO₂ nanoparticles in varying amounts into thermoset matrices will improve the mechanical performance of the composites.

M. Landowski et al. investigated impact damage in epoxy-carbon fiber composites enhanced by SiO₂ nanoparticles. The epoxy resin matrix was augmented with SiO₂ nanoparticles ranging in weight from 1% to 8%, using industrial surface modified nano silicas. Impact characteristics such as force, deformation, energy, and damage extent were recorded. The most noticeable consequence of these factors is a reduction in damage size. For example, infrared thermography and X-ray computed radiography detected a 28% drop in the composite containing 8% nano SiO₂. Crack branching and deflection produced by nanoparticles were discovered. Approximately 15% permanent deformation and 8% reduction in energy absorption were found, as well as an increase in fiber/matrix interface strength.

The flexural strength peaked at 640 MPa at 2-5% nano- SiO₂ concentration and thereafter dropped, most likely because to nanoparticle aggregation. A 6% increase in peak impact force was observed in the composite containing 8% nano- SiO₂. The commencement of a drop in maximum power and impact damage size was discovered for 5% nano- SiO₂. An significant 28% decrease in damage size was reported in the composite containing 8% nano- SiO₂. The lack of previous reports of such a significant reduction in damage size for glass fiber reinforced plastic (GFRP) and carbon fiber reinforced plastic (CFRP) laminates has been attributed to energy absorption mechanisms provided by crack deflection and crack branching caused by nanoparticle agglomerates (Landowski, et al., 2017).

In this study, hybrid epoxy composites reinforced with glass, carbon, and aramid fibers were produced due to their high strength and lightweight characteristics widely utilized in engineering applications. Hybrid composites with different fiber stacking sequences (CAG, AGC, and GCA) were fabricated, and the effect of adding 2 wt% TiO₂ particles on their mechanical properties was investigated.

Tensile, flexural, and quasi-static penetration tests were conducted on the specimens, and the results revealed that TiO₂ addition improved the strength of all hybrid sequences. The highest enhancement was observed in the GCA sequence, while in the CAG sequence, which contains carbon fiber, the mechanical strength increased by approximately 6% with the addition of 2 wt% TiO₂. Overall, the inclusion of TiO₂ particles was found to be effective in enhancing the mechanical performance of hybrid epoxy nanocomposites (Alptekin, 2022).

In this work, the effects of different TiO₂ particle ratios (0%, 1%, 2%, and 5%) on the mechanical properties of glass fiber reinforced polymer (GFRP) composites were investigated. Based on tensile, impact, flexural, and SEM analyses, it was observed that the addition of TiO₂ particles enhances mechanical strength up to a certain level, with the optimum performance achieved at 1% TiO₂ content. Particularly, the 1% TiO₂-reinforced GFRP specimens exhibited a more homogeneous structure, better particle distribution, and superior mechanical properties, especially in impact, flexural, and tensile strength (Seshu kamal, et al., 2025).

This study will look at how adding a combination of SiO₂ and TiO₂ (with an equal ratio of SiO₂ to TiO₂) in varying quantities to diverse samples affects the mechanical characteristics of thermoset matrix composites. Mechanical qualities such as tensile strength and impact resistance will be investigated experimentally, offering a full

understanding of how to optimize nanomaterial reinforcement for optimum performance.

The purpose of this work is to contribute to the development of high-performance composite materials by determining the impact of SiO₂ and TiO₂ nanoparticles on the mechanical characteristics of thermoset matrix composites. In this regard, the goal is to give substantial insights into how nanomaterial-enhanced composites might be used in future applications.

The materials and techniques section will go into depth about the composites' preparation and test procedures. The findings and discussion sections will describe and explain the acquired results, while the conclusion will synthesize them and make recommendations for future study.

In this work, nano titanium dioxide (TiO₂) particles were introduced to the epoxy matrix carbon fiber composite at 0%, 2%, 4%, and 6% mass concentrations. The generated samples were tested for impact and wear resistance. Carbon fibers have a more brittle structure than other synthetic fibers. As a result, its usage is limited in applications that need strong impact resistance. However, the inclusion of TiO₂ particles significantly improved the composites' impact strength. The inclusion of nanoparticles filled the voids inside the samples, increasing the adhesion between the epoxy and fiber material. The results of the testing revealed that the inclusion of TiO₂ improved the mechanical characteristics of the composites. Composite samples with 4% nano TiO₂ particles demonstrated the greatest improvement. (Al-Zubaydi, et al., 2021)

In this investigation, SiO₂ nanoparticles were combined with epoxy fiber glass composites in varying quantities. Tensile testing was performed on composite samples made by combining SiO₂ particles at 0%, 1%, 3%, and 5% by mass. Nanoparticles were shown to increase the adhesion force between fibers and matrices, as well as the mechanical characteristics of the samples. The sample with the best tensile strength was the one containing 1% SiO₂. Furthermore, samples with larger particle concentrations generated aggregation in the matrix, reducing material strength. The study investigated composites with plies organized in various orientations, and composites with plies parallel to the tensile direction demonstrated increased tensile strength. (Tuncer, et al., 2022)

Previous research has demonstrated that SiO₂ and TiO₂ nanoparticles enhance the mechanical characteristics of composite materials. Given the impact resistance enhancement of TiO₂ particles on the composite and the good effect of SiO₂ on tensile strength, it is predicted that the combined action of these two particles will result in a two-sided improvement in the composite material created.

Although several studies have examined the individual effects of SiO₂ or TiO₂ microparticles on composite behavior, the synergistic influence of their combined use in carbon fiber-reinforced thermoset matrices has not been sufficiently investigated. In this study, composites with an optimized ply orientation were produced, and the effects of adding SiO₂-TiO₂ microparticles at different concentrations on the tensile and impact performance were experimentally evaluated. By identifying the particle content

that enhances mechanical strength without causing aggregation-related defects, this work is intended to provide a novel contribution to the engineering of high-performance hybrid microparticle-reinforced composites for advanced structural applications.

2. MATERIALS AND METHODS

2.1. Materials

MGS LR285 and MGS LH285 were used as the epoxy resin, the hardener respectively, and microparticles of SiO₂ and TiO₂ with the sizes of 10µm and 0,4µm respectively were chosen as reinforcement. Physical properties of epoxy and hardener at 25oC are given in given in Table. Unidirectional carbon fiber with the laminae weight of 646 g/m², thickness of 0,48 mm, and having a resin consumption of 346 g/m² was used in laminate fabrication.

Table 1. Physical Properties of Resin and Curing Agent

	Epoxy Resin MGS LR285	Curing Agent MGS LH285
Density [g/cm ³]	1,18-1,23	0,94-0,97
Viscosity [mPa·s]	600-900	50-100
Refractory index	1,525-1,530	1,500-1,510

2.2. Optimization of Ply Orientation

To obtain the greatest results from the tensile and impact tests, the plies should be stacked symmetrically with respect to the mid-plane to provide a stable laminate structure. Secondly, to achieve high elastic modulus in both the x and y directions, the plies should be placed at 90°, 0°, and 45° angles. Additionally, plies with the same angle should not be placed consecutively. Taking these factors into account, laminates with 10 different stacking sequences were evaluated in MATLAB using the Tsai-Wu criterion and a 1 kN tensile force in the y direction (the direction parallel to the fibers in the 0° ply).

Table 2. Different Angle Orientations According to Types

Code	Orientations
A	[0° / +45° / -45° / 90° / 0° / 90° / -45° / +45° / 0°]
B	[90° / +45° / -45° / 0° / 90° / 0° / -45° / +45° / 90°]
C	[-45° / 0° / +45° / 90° / -45° / 90° / 45° / 0° / -45°]
D	[0° / -45° / 90° / +45° / 0° / +45° / 90° / -45° / 0°]
E	[-45° / 90° / +45° / 0° / -45° / 0° / +45° / 90° / -45°]
F	[90° / -45° / 0° / +45° / 90° / +45° / 0° / -45° / 90°]
G	[+45° / -45° / 90° / 0° / +45° / 0° / 90° / -45° / +45°]
H	[90° / -45° / 0° / +45° / 90° / +45° / 0° / -45° / 90°]
I	[0° / +45° / 90° / -45° / 0° / -45° / 90° / +45° / 0°]
J	[+45° / 0° / 90° / -45° / +45° / -45° / 90° / 0° / +45°]

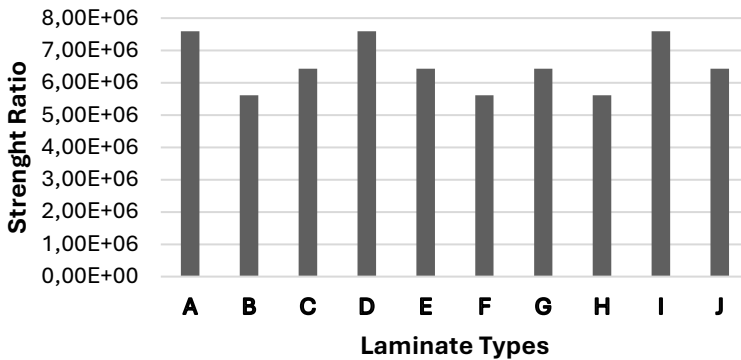


Figure 1. Strength Ratios of Each Laminate

The Tsai-Wu failure criteria were applied to each laminate, and the one with the greatest SR value was chosen. Laminate A was determined to be the most suited for manufacturing considering the strength ratios.

2.3. Production Methods

2.3.1. Vacuum bagging method

During the curing step, the laminate is mechanically compressed using vacuum bagging. Applying pressure to composite laminates can offer several advantages. First, it removes trapped air between layers. Second, it keeps the fibers aligned when curing and compresses the fiber layers to guarantee proper force transmission between fiber bundles. Third, it lowers humidity. Most notably, vacuum bagging improves the fiber-to-resin ratio in the composite product. These benefits have long enabled the racing and aerospace sectors to enhance the physical qualities of modern composite materials like carbon, aramid, and epoxy (Irisarri, et al., 2014; Dangsheng, 2005; Molazemhosseini, et al., 2013; Stoeffler, 2013).

2.3.2. Production of specimens

A total of four composite specimens were fabricated for this study. %0,5SiO₂ + %0,5TiO₂, %1 SiO₂ + %1SiO₂, and %2SiO₂ + %2TiO₂ were the ratios at which microparticles were introduced to the epoxy resin selected as the matrix. Furthermore, one of the specimens was made without microparticle addition. For microparticle-reinforced composite materials, the necessary weight of particles was first mixed with the resin and then sonicated in an ultrasonic bath. Sonication homogenizes the mixture, removes air bubbles, reduces viscosity, accelerates curing, and improves microparticle functioning. These techniques allow for improved microparticle dispersion within the epoxy matrix, which improves the mechanical properties of composites. Prior to application of matrix phase onto fiber mats, the hardener is added and mixed homogeneously followed by curing under vacuum for 24 hours.

In the first step of fabrication, the carbon fiber fabric was cut to the required sizes, as shown in Figure 2. The illustration shows 130 mm fabric for 0- and 90- degree plies, whereas the 195 mm fabric is for 45- degree plies.

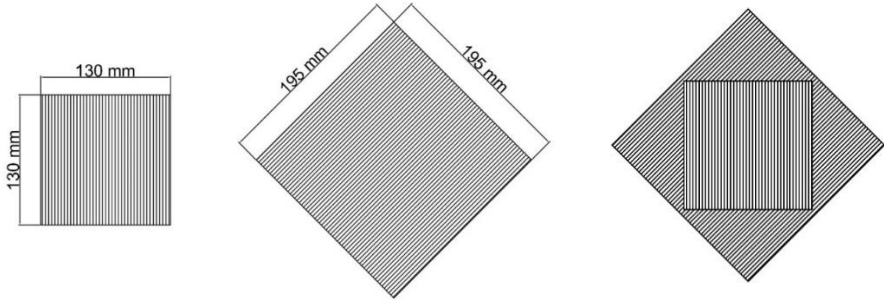


Figure 2. Stacking Carbon Fiber Mats.

The cut carbon fiber fabrics are arranged properly on the metal table can be seen in Figure 3. The prepared epoxy/hardener mixture with predefined microparticle combination is applied evenly to each layer of carbon fiber, resulting in a total of nine layers.

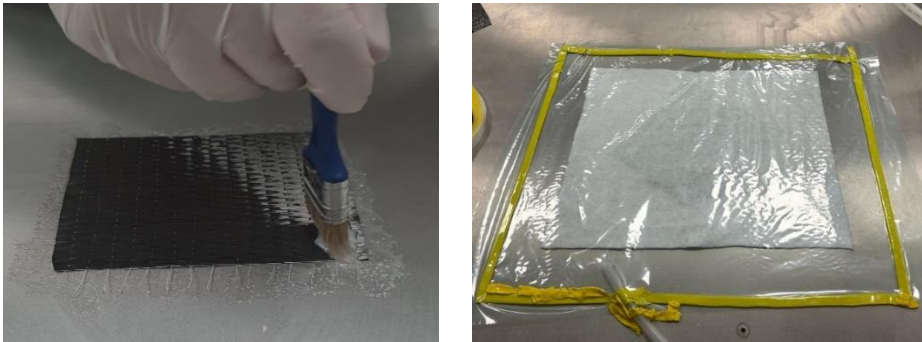


Figure 3. Application of Epoxy-Hardener Mixture on Each Ply.

2.4. Test Methods

2.4.1. Tensile test

The ultimate tensile strength, strain at the ultimate strength point and elastic modulus of carbon/epoxy composites were investigated by tensile test in Figure 4. The test was performed employing the Shimadzu testing machine in accordance with ASTM D638. The specimens were in dog-bone shape, measuring 115 mm long, 19 mm wide, and 3 mm thick. The test speed of 2,5 mm/min was chosen for all the test specimens.



Figure 4. The Setup of the Tensile Test

2.4.1. Charpy impact test

The Charpy Impact test is used to determine how materials respond to impact energy. This test allows for determination of the fracture strength, ductility, and brittleness characteristics of a material. The test was conducted using an INSTRON impact pendulum in accordance with ASTM E23. The specimens were rectangular in shape, measuring 55 mm long, 10 mm wide, 3 mm thick, and with a notch length of 2 mm. For test specimens, an impact velocity of 3,799 m/s and a potential hammer energy of 15 J are applied. To calculate the Charpy Impact Strength, the formula below was employed.

$$C_{VN} = \frac{E}{(B - a)t} \times 10^3$$

where B is the width of the specimen (mm), a is the notch length of specimen (mm), t is the thickness of specimen (mm), and E is the absorbed Energy (Joule).

3. RESULTS AND DISCUSSIONS

3.1. Tensile Test Results

Tensile test results are calculated using the force versus stroke graphs provided for each specimen. Following that, the stroke strain was transformed into the stress versus strain diagram (Fig 5.). The yield strengths of the material were determined using the stress-strain graph and the 0,2 percent method. The graphic shows the ultimate tensile strength as the maximum point.

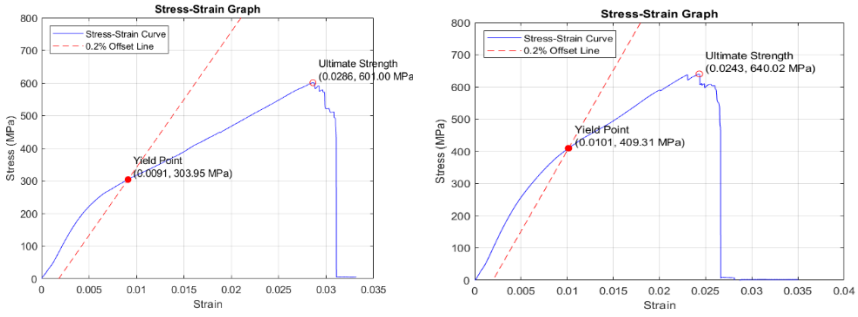


Figure 5. Stress–Strain Graphs for Composites with 0% and 1% Particle Weight Fractions, Respectively

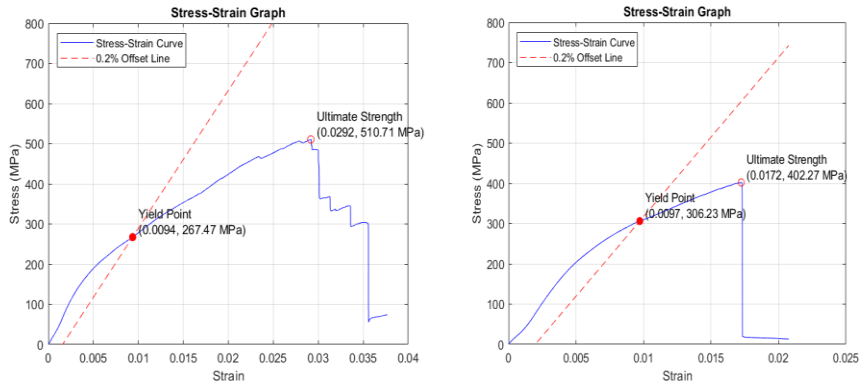


Figure 6. Stress–Strain Graphs for Composites with 2% and 4% Particle Weight Fractions, Respectively

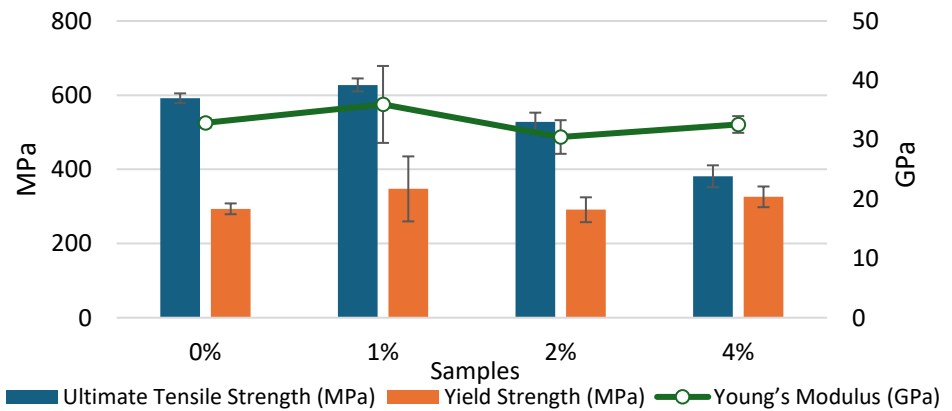


Figure 7. Average Tensile Strength Properties of Composite Samples

As can be seen from Figure 7, results from tensile and Charpy impact tests showed that the addition of SiO₂-TiO₂ particles significantly affected the mechanical behavior of thermoset matrix composites. It was aimed to see how the mechanical characteristics would alter in the tests run by increasing the particle mass ratio in each sample when the specimens are subjected to the tensile test. In comparison to the sample with 0% particle addition, the ultimate tensile strengths changed by +4,33%, -12,15%, and -45,34% for the samples with 1%, 2% and 4% particle addition respectively. The improvement observed with the addition of 1% particles indicates that the particles were effectively dispersed within the epoxy matrix and strengthened the interfacial bond between the matrix and the fibers. This result is consistent with previous findings in the literature, where optimum particle contents around 1–2% were reported to increase mechanical strength by improving load transfer efficiency and limiting microcrack propagation (Suresha, et al., 2021; Tuncer, et al., 2022).

This situation is attributed to the aggregation of particles. Aggregation in composites with a high particle-to-mass ratio might have developed because the particles might have not dispersed homogeneously. This degradation leads to heterogeneous particle distribution within the matrix and the formation of microvoids. These agglomerated regions act as stress concentrators, causing premature failure under tensile load. A similar behavior was reported by Landowski et al. (2017), who observed that mechanical performance decreased at higher SiO₂ concentrations due to aggregation-induced defects. Therefore, it can be concluded that there is a critical particle concentration above which the reinforcing effect of particles diminishes. As a result, these aggregations formed in composite structure act as stress concentrator points and lower the mechanical properties of materials.

Charpy impact test results revealed that when carbon fiber composite is constructed using an epoxy mixture that contains SiO₂ and TiO₂ particles, it inhibits the development of microcracks in the particle matrix and offers impact resistance that will hinder the progression of ripping in the cracks. The impact resistance of the composite is increased by the particles' strong interfacial contact with the epoxy (Molazemhosseini, et al., 2013). Samples containing 1%, 2%, and 4% particle additions showed changes in impact strength of +12,6%, -0,5%, and -7,5%, respectively, compared to the sample containing 0% particle addition. The highest impact strength was achieved in the 1 wt% sample, which demonstrated enhanced energy absorption capacity due to strong interfacial adhesion and effective crack deflection mechanisms. These particles improved matrix toughness and fiber–matrix interlocking, preventing microcrack initiation and propagation.

The sample with the most ductile characteristics when it comes to crack propagation resistance is seen to be the sample with 1% particle concentration. In this instance, the specimen with the most brittle characteristic is sample with 4% particle concentration. This might be attributed to agglomeration of particles in the epoxy mixture at high proportions which caused the composite to become less homogeneous and create stress concentration points. At higher particle concentrations (≥ 2 wt%), excessive agglomeration reduced the homogeneity of the composite and promoted brittle fracture behavior. The 4 wt% sample exhibited the most brittle properties with visible crack propagation paths, confirming the negative impact of particle aggregation on impact energy absorption. These findings are consistent with previous studies showing that

particle overload can lead to embrittlement of the epoxy matrix due to reduced matrix continuity and increased hardness (Tutunchi, et al., 2015; Molazemhosseini, et al., 2013).

All in all, total Charpy impact resistance of samples containing 1%, 2% and 4% particle mixture changed by +12,6%, -0,5%, -7,5% respectively compared to the 0% particle added sample. Overall, both tensile and impact test results indicate that the combined use of SiO₂ and TiO₂ particles improves the mechanical performance of the composites up to an optimum concentration of approximately 1 wt%. Beyond this limit, aggregation-induced defects negate these advantages. This result supports the hypothesis proposed in the introduction that the synergistic effect of SiO₂ and TiO₂ particles, when adequately dispersed, can simultaneously enhance tensile and impact properties. Therefore, controlling particle dispersion during composite fabrication is critical to achieving the desired balance between strength and toughness in advanced thermoset matrix composites.

3.2. Theoretical Results of Tensile Properties

The Mechanical Properties of a unidirectional lamina (Table 3) found in the technical documents of the carbon-fiber used are processed in MATLAB code and what the Mechanical Properties of a Unidirectional Lamina will be if the laminates are arranged in the determined orientation (code A) is stated in the tables below.

Where mechanical properties are:

Table 3. Mechanical Properties of Epoxy/Carbon Fiber Composite

Mechanical Properties	Metric
Longitudinal elastic modulus (GPa)	70-75
Transverse elastic modulus (GPa)	5,5-6,5
Poisson's ratios	0,28
Shear modulus (GPa)	5-6
Ultimate longitudinal tensile strength (MPa)	600-750
Ultimate longitudinal compressive strength (MPa)	20-30
Ultimate transverse tensile strength (MPa)	100-150
Ultimate in-plane shear strength (MPa)	30-40

Table 4. Midplane Strains and Curvatures

ϵ_{0x}	ϵ_{0y}	ϵ_{0z}	κ_z	κ_z	κ_x
1,0964×10-9	-2,8555×10-10	0	0	0	0

Table 5. Elastic Constants for This Laminate

E1	E2	Gxy	vxy	vyx
33,78 GPa	26,96 GPa	10,87 GPa	2,6045×10-1	2,0786×10-1

Table 6. Global Stresses (Pa)

Ply no.	Position	σ_x	σ_y	τ_{xy}
1 (0o)	Top	$7,6779 \times 101$	$1,1862 \times 10^{-1}$	0
	Bottom	$7,6779 \times 101$	$1,1862 \times 10^{-1}$	0
2 (+45o)	Top	$2,2937 \times 101$	$9,1177 \times 100$	0
	Bottom	$2,2937 \times 101$	$9,1177 \times 100$	0
3 (-45o)	Top	$2,2937 \times 101$	$9,1177 \times 100$	0
	Bottom	$4,2837 \times 101$	$-2,2967 \times 101$	0
4 (90o)	Top	$4,2837 \times 100$	$-1,8413 \times 100$	0
	Bottom	$4,2837 \times 100$	$-1,8413 \times 100$	0
5 (0o)	Top	$7,6779 \times 101$	$1,1862 \times 10^{-1}$	0
	Bottom	$7,6779 \times 101$	$1,1862 \times 10^{-1}$	0
6 (90o)	Top	$4,2837 \times 101$	$-2,2967 \times 101$	0
	Bottom	$1,9927 \times 101$	$1,1539 \times 101$	0
7 (-45o)	Top	$2,2937 \times 101$	$9,1177 \times 100$	0
	Bottom	$2,2937 \times 101$	$9,1177 \times 100$	0
8 (+45o)	Top	$2,2937 \times 101$	$9,1177 \times 100$	0
	Bottom	$2,2937 \times 101$	$9,1177 \times 100$	0
9 (0o)	Top	$7,6779 \times 101$	$1,1862 \times 10^{-1}$	0
	Bottom	$7,6779 \times 101$	$1,1862 \times 10^{-1}$	0

Table 7. Global Strains

Ply no.	Position	ϵ_x	ϵ_y	γ_{xy}
1 (0o)	Top	$1,0964 \times 10^{-9}$	$-2,8555 \times 10^{-10}$	0
	Bottom	$1,0964 \times 10^{-9}$	$-2,8555 \times 10^{-10}$	0
2 (+45o)	Top	$1,0964 \times 10^{-9}$	$-2,8555 \times 10^{-10}$	0
	Bottom	$1,0964 \times 10^{-9}$	$-2,8555 \times 10^{-10}$	0
3 (-45o)	Top	$1,0964 \times 10^{-9}$	$-2,8555 \times 10^{-10}$	0
	Bottom	$1,0964 \times 10^{-9}$	$-2,8555 \times 10^{-10}$	0
4 (90o)	Top	$1,0964 \times 10^{-9}$	$-2,8555 \times 10^{-10}$	0
	Bottom	$1,0964 \times 10^{-9}$	$-2,8555 \times 10^{-10}$	0
5 (0o)	Top	$1,0964 \times 10^{-9}$	$-2,8555 \times 10^{-10}$	0
	Bottom	$1,0964 \times 10^{-9}$	$-2,8555 \times 10^{-10}$	0
6 (90o)	Top	$1,0964 \times 10^{-9}$	$-2,8555 \times 10^{-10}$	0
	Bottom	$1,0964 \times 10^{-9}$	$-2,8555 \times 10^{-10}$	0
7 (-45o)	Top	$1,0964 \times 10^{-9}$	$-2,8555 \times 10^{-10}$	0
	Bottom	$1,0964 \times 10^{-9}$	$-2,8555 \times 10^{-10}$	0
8 (+45o)	Top	$1,0964 \times 10^{-9}$	$-2,8555 \times 10^{-10}$	0
	Bottom	$1,0964 \times 10^{-9}$	$-2,8555 \times 10^{-10}$	0
9 (0o)	Top	$1,0964 \times 10^{-9}$	$-2,8555 \times 10^{-10}$	0
	Bottom	$1,0964 \times 10^{-9}$	$-2,8555 \times 10^{-10}$	0

Table 8. Local Stresses (Pa)

Ply no.	Position	σ_1	σ_2	τ_{12}
1 (0o)	Top	$7,6779 \times 10^1$	$1,1862 \times 10^{-1}$	0
	Bottom	$7,6779 \times 10^1$	$1,1862 \times 10^{-1}$	0
2 (+45o)	Top	$2,9183 \times 10^1$	$2,8718 \times 10^0$	$-6,9096 \times 10^0$
	Bottom	$2,9183 \times 10^1$	$2,8718 \times 10^0$	$-6,9096 \times 10^0$
3 (-45o)	Top	$2,9183 \times 10^1$	$2,8718 \times 10^0$	$6,9096 \times 10^0$
	Bottom	$2,9183 \times 10^1$	$2,8718 \times 10^0$	$6,9096 \times 10^0$
4 (90o)	Top	$-1,8413 \times 10^1$	$5,6249 \times 10^0$	0
	Bottom	$-1,8413 \times 10^1$	$5,6249 \times 10^0$	0
5 (0o)	Top	$7,6779 \times 10^1$	$1,1862 \times 10^{-1}$	0
	Bottom	$7,6779 \times 10^1$	$1,1862 \times 10^{-1}$	0
6 (90o)	Top	$-1,8413 \times 10^1$	$5,6249 \times 10^0$	0
	Bottom	$-1,8413 \times 10^1$	$5,6249 \times 10^0$	0
7 (-45o)	Top	$2,9360 \times 10^1$	$2,1050 \times 10^0$	$6,9096 \times 10^0$
	Bottom	$2,9360 \times 10^1$	$2,1050 \times 10^0$	$6,9096 \times 10^0$
8 (+45o)	Top	$2,9360 \times 10^1$	$2,1050 \times 10^0$	$-6,9096 \times 10^0$
	Bottom	$2,9360 \times 10^1$	$2,1050 \times 10^0$	$-6,9096 \times 10^0$
9 (0o)	Top	$7,6779 \times 10^1$	$1,1862 \times 10^{-1}$	0
	Bottom	$7,6779 \times 10^1$	$1,1862 \times 10^{-1}$	0

Table 9. Local Strains

Ply no.	Position	ϵ_1	ϵ_2	γ_{12}
1 (0o)	Top	$1,0964 \times 10^{-9}$	$-2,8555 \times 10^{-10}$	0
	Bottom	$1,0964 \times 10^{-9}$	$-2,8555 \times 10^{-10}$	0
2 (+45o)	Top	$4,0541 \times 10^{-10}$	$4,0541 \times 10^{-10}$	$-1,3819 \times 10^{-9}$
	Bottom	$4,0541 \times 10^{-10}$	$4,0541 \times 10^{-10}$	$-1,3819 \times 10^{-9}$
3 (-45o)	Top	$4,0541 \times 10^{-10}$	$4,0541 \times 10^{-10}$	$1,3819 \times 10^{-9}$
	Bottom	$4,0541 \times 10^{-10}$	$4,0541 \times 10^{-10}$	$1,3819 \times 10^{-9}$
4 (90o)	Top	$-2,8555 \times 10^{-10}$	$1,0964 \times 10^{-9}$	0
	Bottom	$-2,8555 \times 10^{-10}$	$1,0964 \times 10^{-9}$	0
5 (0o)	Top	$1,0964 \times 10^{-9}$	$-2,8555 \times 10^{-10}$	0
	Bottom	$1,0964 \times 10^{-9}$	$-2,8555 \times 10^{-10}$	0
6 (90o)	Top	$-2,8555 \times 10^{-10}$	$1,0964 \times 10^{-9}$	0
	Bottom	$-2,8555 \times 10^{-10}$	$1,0964 \times 10^{-9}$	0
7 (-45o)	Top	$4,0541 \times 10^{-10}$	$4,0541 \times 10^{-10}$	$1,3819 \times 10^{-9}$
	Bottom	$4,0541 \times 10^{-10}$	$4,0541 \times 10^{-10}$	$1,3819 \times 10^{-9}$
8 (+45o)	Top	$4,0541 \times 10^{-10}$	$4,0541 \times 10^{-10}$	$-1,3819 \times 10^{-9}$
	Bottom	$4,0541 \times 10^{-10}$	$4,0541 \times 10^{-10}$	$-1,3819 \times 10^{-9}$
9 (0o)	Top	$1,0964 \times 10^{-9}$	$-2,8555 \times 10^{-10}$	0
	Bottom	$1,0964 \times 10^{-9}$	$-2,8555 \times 10^{-10}$	0

When the theoretically obtained E1 value of 33,78 GPa is compared with the Longitudinal Young's Modulus of 33,4 GPa of the specimen with 0% particles, a

difference of -1% is observed. In this case, the local and global stress strain values shown in the tables can be evaluated with a tolerance of 1%.

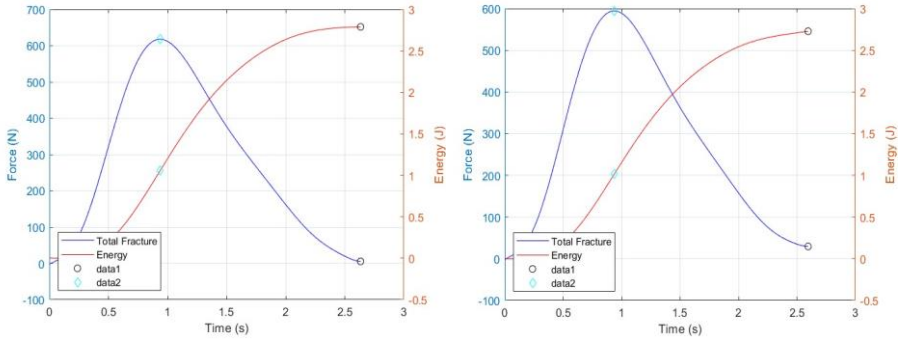


Figure 8. Time vs Force and Energy Graphs for Two Samples Of 0% Mixture Ratio

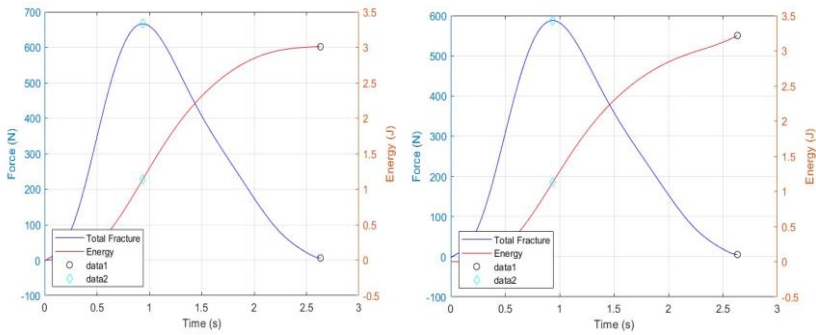


Figure 9. Time vs Force and Energy Graphs for Two Samples Of 1% Mixture Ratio

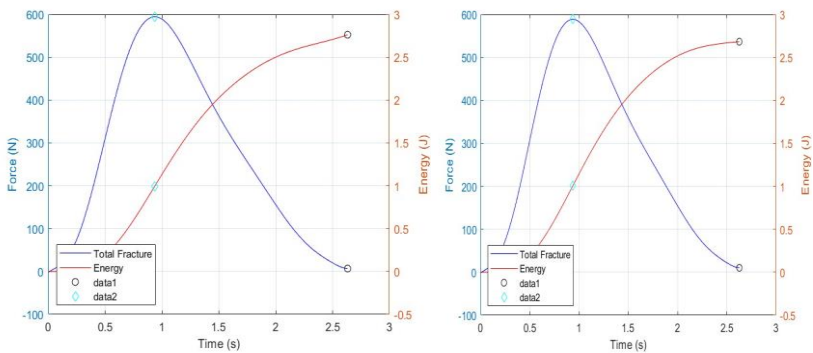


Figure 10. Time vs Force and Energy Graphs for Two Samples Of 2% Mixture Ratio

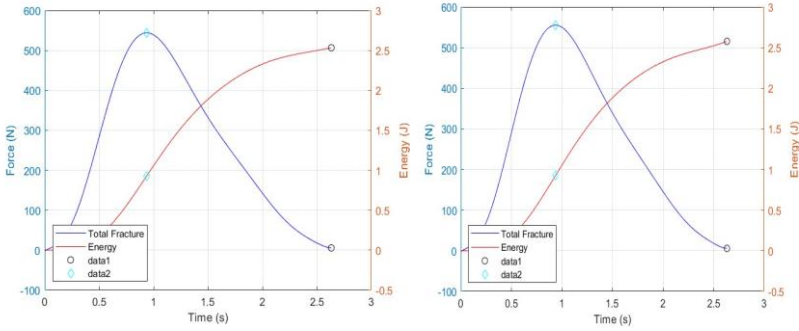


Figure 11. Time vs Force and Energy Graphs for Two Samples Of 4% Mixture Ratio

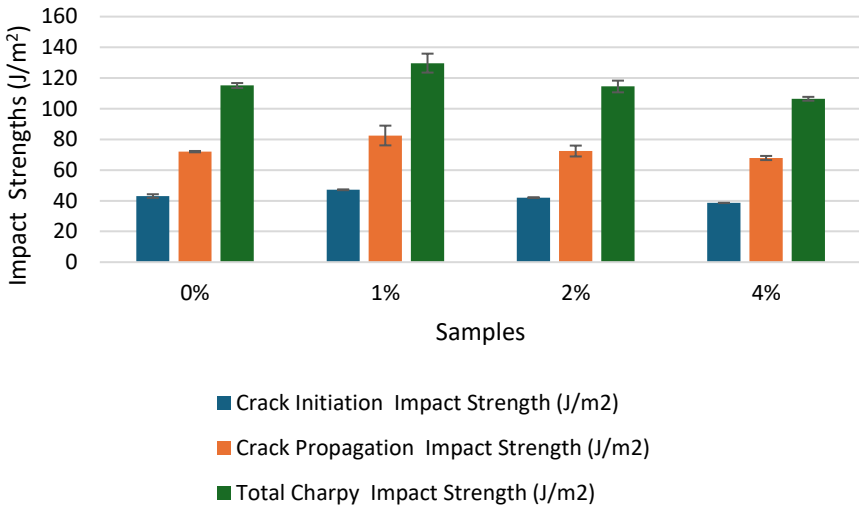


Figure 12. Average Impact Strength Properties of Composite Samples

4. CONCLUSION

Carbon-fiber epoxy composites with four different microparticle concentrations have been produced for the purpose of this research. These composites were compared in various laminate sequences to optimize their orientation, and the proper ply $[0^\circ / +45^\circ / -45^\circ / 90^\circ / 0^\circ / 90^\circ / -45^\circ / +45^\circ / 0^\circ]$ was discovered. After testing microparticle-free and microparticle-containing composites with varying mass ratios, the effects of the microparticle ratio on the mechanical characteristics of the composite were investigated. Tensile and Charpy impact tests were used to investigate their effects on mechanical characteristics. The composite with 1% SiO₂-TiO₂ particles performed the best in the tensile test; in other words, its Ultimate Tensile Strength increased by 4,33% when compared to the composite without microparticles. In contrast to the composite with no microparticles, the mechanical characteristics of the composites with 2% and 4% microparticles were found to be reduced. The addition of microparticles to the composites improved their impact resistance in the impact test by

inhibiting the development of microcracks and hindering their spread. The most brittle characteristics are seen in Sample 4, whereas the most ductile characteristics are found in Sample 2. This can be because the composite's homogeneity is being disrupted by the high particle ratio. In comparison to the sample with no particle addition, the total Charpy strengths changed by +12,6%, -0,5%, and -7,5%, respectively. It was shown that when the ratio of epoxy to microparticles was higher than ideal, the mechanical qualities of the resulting composites dramatically declined.

Authors' Contributions

A.U.; methodology, A.U. and M.C.; software, M.E.A.; validation, A.U. and M.C.; formal analysis, F.G.O.; investigation, G.O.; resources, A.U. and M.C.; experimental work, G.O. , M.E.A. and F.G.O.; data curation, A.U.; writing—original draft preparation, M.E.A. and G.O.; writing—review and editing, G.O.; visualization, F.G.O.; supervision, A.U. and M.C.; project administration, A.U. All authors have read and agreed to the published version of the manuscript.

Conflict of Interest Statement

There is no conflict of interest among the authors.

Research and Publication Ethics Statement

Research and publication ethics were followed in the study.

REFERENCES

- Alptekin A., (2022). Tio2 nano partikül katkılı cam, aramid, karbon hibrit epoksi kompozitlerin mekanik özellikleri.
- Al-Zubaydi, A.S.J. Salih, R.M. & Al-Dabbagh, B. M. (2021). Effect of nano TiO2 particles on the properties of carbon fiber-epoxy composites. *Progress in Rubber Plastics and Recycling Technology*, 37(3) 216–232.
- Dangsheng, X. (2005). Friction and wear properties of UHMWPE composites reinforced with carbon fibers. *Mater Lett*, 59, 175–179. 7.
- Han, F. Yan, Y. Ma, J., (2016). Experimental Study and Progressive Failure Analysis of Stitched Foam-core Sandwich Composites Subjected to Low-velocity Impact, *Polym. Compos.* 39(3), 624–635.
- Heutling, F. Franz, H. E. & Friedrich K. (1998). Photomicrographic fracture analysis of the delamination propagation in cyclic loaded thermosetting carbon fiber-reinforced composites, *Materialwissenschaften und Werkstofftechnik* 29, 239 (in German).
- Irisarri, F., Lasseigne, A., Leroy, F., & Le Riche, R. (2014). Optimal design of laminated composite structures with ply drops using stacking sequence tables. *Composite Structures*, 559-564.
- Kandelbauer, P. (2014), InHandbook of Thermoset Plastics, 3rd ed.; Dodiuk, H., Goodman, S. H., Eds.; WilliamAndrew, 739– 753.

- Kim, B.C. Park, S.W. & Lee, D.G. (2008). Fracture toughness of the nano particle reinforced epoxy composite, *Compos. Struct.* 86, 69–77.
- Landowski, M. Strugala, G. & Budzik M. (2017). Impact damage in SiO₂ nanoparticle enhanced epoxy – Carbon fibre composites.
- Molazemhosseini A, Tourani H, Khavandi A, et al. (2013) Tribological performance of PEEK based hybrid composites reinforced with short carbon fibers and nano silica. *Wear* 303(1–2), 397–404. 8.
- Muda, M. K. H., & Mustapha, F. (2018). Composite patch repair using natural fiber for aerospace applications, sustainable composites for aerospace applications. *Sustainable Composites for Aerospace Applications*, 171-209. Woodhead Publishing.
- Rong Z, Sun W, Xiao H, Jiang G. (2015). Effects of nano-SiO₂ particles on the mechanical and microstructural properties of ultra-high performance cementitious composites. *Cement and Concrete Composites*, 56, 25-31.
- Seshu kamal, M., Prasad, T., E Nirmala Devi, M. Srinivasa Rao, G. Ramakrishna (2025). Mechanical properties and evaluation of glass fiber reinforced polymer/ TiO₂ nano composite laminates.
- Stoeffler K, Andjelic S, Legros N, et al. (2013). Polyphenylene sulfide (PPS) composites reinforced with recycled carbon fiber. *Compos Sci Technol*, 84, 65–71.
- Suresha, B. Divya, G.S. Hemanth G. & Somashekar H.M. (2021). Physico-Mechanical Properties of Nano Silica-Filled Epoxy- Based Mono and Hybrid Composites for Structural Applications.
- Tuncer, C., Canyurt, O.E. (2022). The strength of glass fiber composite materials by inclusion of CaCO₃ and SiO₂ nanoparticles into resin 2022; *Pamukkale Univ Muh Bilim Derg*, 28(4), 493-498.
- Tutunchi A, Kamali R and Kianvash A. (2015). Steel–epoxy composite joints bonded with nano TiO₂ reinforced structural acrylic adhesives. *J Adhes* 91(9), 663–676.
- Wang, J. Waas, A.M. Wang, H. (2013) Experimental and numerical study on the low velocity impact behavior of foam-core sandwich panels, *Compos. Struct.* 96 298–311.
- Wetzel, B. Hauptert, F. & Rong M.Z. (2002). Nanoparticle-reinforced composites: preparation, structure, properties, Proc. 81h Natl. Symp. SAMPE, *Deutschland e.V.*, Kaiserslautern (in German).
- Zhang, M. Zeng, H. Zhang, L. Lin, G. Lii R. K. Y. (1993). Fracture characteristics of discontinuous carbon fibre-reinforced PPS and PES-C composites, *Polym. Polym. Compos.* 1,357.